

# What Makes a Scene ? Scene Graph-based Evaluation and Feedback for Controllable Generation

Zuyao Chen  
The Hong Kong Polytechnic University  
zuyao.chen@connect.polyu.hk

Jinlin Wu, Zhen Lei  
Institute of Automation, CAS  
{wujinlin2017, zhen.lei}@ia.ac.cn

Chang Wen Chen  
The Hong Kong Polytechnic University  
changwen.chen@polyu.edu.hk

## Abstract

While text-to-image generation has been widely explored, synthesizing images from scene graphs remains relatively underexplored due to challenges in capturing complex spatial relationships and object interactions. To bridge this gap, we introduce Scene-Bench, a comprehensive benchmark for evaluating and enhancing factual consistency in natural scene generation. Scene-Bench comprises MegaSG, a large-scale dataset of one million images annotated with detailed scene graphs, enabling extensive training and fair comparisons across diverse and intricate scenes. In addition, we propose SGScore, a novel evaluation metric that leverages the reasoning capabilities of multimodal large language models to assess both object presence and relationship accuracy, thereby providing a more precise measure of factual consistency than traditional metrics such as FID and CLIPScore. Furthermore, our scene graph feedback pipeline iteratively refines generated images by identifying and correcting discrepancies between the intended scene graph and the output. Extensive experiments demonstrate that Scene-Bench offers an effective evaluation framework for complex scene generation, and our feedback strategy significantly improves the factual consistency of image generation models, advancing the field of controllable image generation.

## 1. Introduction

“If you can’t measure it, you can’t improve it.”

– Peter Drucker

Generating realistic images coherent with natural scenes is important in numerous applications such as photo editing [25, 29, 73], content creation [4, 28, 52], etc. Early generative models like Variational Autoencoders (VAE) [30]

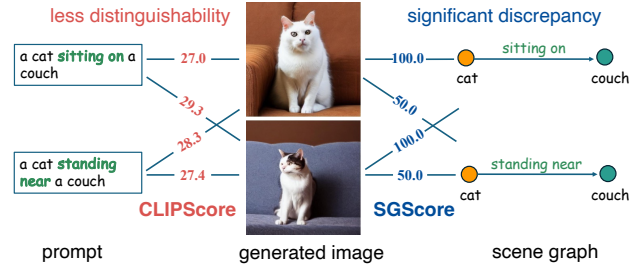


Figure 1. A comparison of CLIPScore [21] and the proposed SGScore for evaluating factual consistency. SGScore can distinguish such relationship discrepancies, while CLIPScore often overlooks them.

produced blurry images due to limitations in modeling complex data distributions. Generative Adversarial Networks (GAN) [19] improved image quality but faced issues like training instability and mode collapse. Recently, diffusion models like Stable Diffusion [52] have proven effective for generating visually appealing images with realistic objects and high-resolution details [14, 23, 45, 48]. Although diffusion models have achieved significant success, they still face challenges in generating complex scenes involving multiple objects [41, 67], particularly in ensuring factual consistency, such as the accurate presence of multiple objects and the correct relationship between objects within a natural image.

Recent efforts have aimed to address these limitations, focusing on compositional objects [17, 42, 43], improving text-image alignment [15, 33], and enhancing spatial consistency [7]. For instance, methods like Composable Diffusion [42] compose multiple concepts by explicitly optimizing the defined energy functions, and Structured Diffusion [17] combines multiple objects by manipulating cross-attention layers. These methods improve the accuracy of

multiple objects occurring in a single scene. Additionally, Chatterjee [7] proposed a benchmark to evaluate and enhance the capability of modeling spatial relationships.

Despite this progress, *how to evaluate the factual consistency between the condition* (e.g., text, image, etc.) *and the generated image* remains challenging. The difficulty lies in standard metrics like Fréchet Inception Distance (FID) [22] and CLIPScore [21] primarily evaluate image quality but fall short in capturing factual consistency in complex scenes. FID, widely used to assess the visual fidelity of generated images, focuses on feature distribution matching between real and generated datasets. However, it overlooks spatial relationships and object interactions. For instance, images depicting a dog “under a table” and “on a table” may receive similar FID scores, despite their vastly different relationships. Similarly, CLIPScore measures semantic alignment between images and text by emphasizing global themes but cannot assess specific object relationships. CLIPScore may assign high scores to images that include all relevant objects but incorrectly depict their relationships, such as confusing “a cat sitting on a couch” with “a cat standing near a couch” (see Fig. 1). The drawback of FID and CLIPScore highlights the need for more specialized evaluation metrics to assess objects’ presence and precise interactions between them.

To evaluate the factual consistency, we employ a structured representation known as a *Scene Graph*, which has been demonstrated to outperform pure text in image retrieval [26, 31]. A scene graph encodes objects as nodes and their relationships as edges. For textual conditions, scene graphs can be parsed using natural language processing tools such as Scene Parser [44] or large language models (LLMs). For image conditions, scene graphs are generated via Scene Graph Generation (SGG) models [11, 58, 64, 70] or multimodal LLMs. Leveraging this structured representation, we introduce a novel evaluation metric, *SGScore*, which quantifies the factual consistency between generated images and their corresponding scene graphs. *SGScore* evaluates *Object Recall* by verifying the presence of nodes and *Relation Recall* by assessing the accuracy of edges within the scene graph. To adapt different domains and handle the extensive vocabulary inherent in generated images, we utilize a multimodal LLM to perform these evaluations instead of relying on a pre-trained SGG model to convert images into scene graphs. Thanks to the reasoning and zero-shot capabilities of the multimodal LLM, *SGScore* can effectively distinguish between images depicting subtle differences, as shown in Fig. 1.

When applying the new metric to benchmark different generative models, a critical bottleneck is the lack of large-scale datasets annotated with scene graphs, which are essential for fair and comprehensive comparisons. Existing datasets, such as Visual Genome (VG) [31] and COCO-

Stuff [6], are relatively small (e.g., only 5k and 2k images for testing, respectively), and their inherent long-tail distributions lead to biased evaluations. As a result, we develop *MegaSG*, a large-scale dataset comprising one million images richly annotated with scene graphs that capture a wide range of objects and their complex relationships. *MegaSG* enables models to be trained and evaluated on diverse scenarios, from simple to highly intricate scenes, thus overcoming the limitations of previous datasets that were constrained by small-scale and biased distributions.

By combining the proposed *SGScore* and *MegaSG*, we introduce a novel benchmark, *Scene-Bench*. To provide a comprehensive and fair benchmark, we sample images from *MegaSG* based on Scene Diversity and Scene Complexity. Scene Diversity sampling aims to evaluate model performance across diverse scene scenarios, while Scene Complexity sampling aims to evaluate model performance at different complexity levels. To our knowledge, *Scene-Bench* is the first benchmark to evaluate generative models on a large-scale natural scene dataset using scene graphs.

Building upon this scene graph-based evaluation, we design a scene graph feedback pipeline that leverages multimodal LLMs for iterative refinement. The process begins with generating an initial image from a scene graph, followed by assessing factual consistency using the *Scene-Bench* metrics. When discrepancies are detected, such as missing objects or incorrect relationships, a missing graph is created to highlight these errors. A reference image is generated based on this missing graph to address the identified issues. By integrating this new image with the initial one, we refine the output, resulting in a final image that more accurately matches the intended scene described by the original scene graph.

In short, our contribution can be summarized as

- We introduce *Scene-Bench*, a comprehensive and large-scale benchmark for evaluating factual consistency in scene graph-to-image generation. *Scene-Bench* includes *MegaSG*, a dataset with one million images annotated with scene graphs, and a novel evaluation metric, *SGScore*, which explicitly measures factual consistency by assessing the accuracy of object presence and relationships in generated images.
- We propose a scene graph feedback strategy that iteratively refines generated images by detecting and correcting discrepancies in object presence and relationship accuracy, thereby enhancing the factual consistency between the generated image and the intended scene.
- Extensive experiments demonstrate that *Scene-Bench* provides a more comprehensive and effective evaluation benchmark for factual consistency in natural scenes. Furthermore, our proposed feedback pipeline significantly improves the factual consistency of generated images, particularly in complex scene scenarios.

## 2. Related Work

**Text-to-Image Generation (T2I).** The field of text-to-image generation has seen significant advancements with the transition from GANs [20] to diffusion models. Early GAN-based methods like StackGAN [71] and AttnGAN [65] generated images from textual descriptions but often struggled with image quality and diversity. The introduction of diffusion models marked a substantial improvement. Models such as DALL-E [50], GLIDE [45], and Stable Diffusion [52] have achieved high-quality image synthesis with better text-image alignment by iteratively refining images from noise, conditioned on text prompts. Despite their success, these models face challenges in generating complex scenes involving multiple objects and ensuring consistency in object relationships.

**Scene Graph-to-Image Generation (SG2IM).** Scene graphs offer a structured representation of objects and their relationships, providing a promising scheme for controllable image generation. Johnson *et al.* [27] introduced SG2Im, a model that generates images from scene graphs using graph convolutional networks (GCN) and conditional GANs. Ashual and Wolf [3] extended this approach by incorporating more detailed scene representations and object attributes. Recent methods have integrated scene graphs with diffusion models to enhance compositionality [16, 40, 42, 56, 62]. However, these approaches often require training on large-scale scene graph datasets and rely on additional guidance like bounding boxes (*e.g.*, [16]) or specialized graph encoders (*e.g.*, [66]), which cannot be adapted to open-vocabulary scenarios. More importantly, evaluating these models remains challenging due to the lack of metrics that effectively capture scene-level fidelity, including object presence and relationship accuracy in generated images.

**LLMs in Image Generation.** The integration of LLMs has opened new possibilities in image generation. Recent works [18, 37, 63, 67] have leveraged LLMs to enhance compositionality and controllability in image synthesis. For example, LayoutGPT [18] utilizes LLMs as visual planners to generate layouts from textual descriptions, improving user controllability. Similarly, methods like RPG [67] and Complex Diffusion [41] leverage the reasoning capabilities of LLMs to decompose complex prompts into simpler tasks, aiding in the generation of complex scenes with multiple objects and relationships. However, their potential for providing feedback to iteratively refine scene graph-based generation has not been fully explored.

**Improving Relationship Consistency.** Addressing the limitations in capturing object relationships, several approaches have been proposed. Feng *et al.* [17] focused on improving compositional generalization in diffusion models through a modulated cross-attention mechanism. Park *et al.* [47] introduced benchmarks specifically targeting compositional understanding in generative models. Chatterjee

Dataset	Images	Obj./Rel.	Test		
			Samples	Triplets	Balanced
VG [31]	108k	179 / 49	5,096	12.8k	✗
COCO-Stuff [6]	4.5k	171 / 6	2,048	22.7k	✗
MegaSG	1M	775 / 122	50,000	275k	✓

Table 1. Comparison of MegaSG with widely-used scene graph datasets. “Obj./Rel.” denotes the number of object and relationship categories, while “Balanced” indicates whether the dataset is balanced with respect to scene complexity. The VG statistics follow the pioneering work [27] in SG2IM, and almost all subsequent works adopt this setting.

*et al.* [7] designed a benchmark to evaluate the capability of modeling spatial relationships. Despite these efforts, ensuring accurate depiction of relationships in complex scenes remains a significant challenge, and existing methods often do not provide mechanisms for iterative refinement based on explicit relationship feedback.

## 3. Scene-Bench

Scene-Bench is a comprehensive benchmark that evaluates and enhances the factual consistency of natural scene generation from scene graphs by rigorously verifying both object presence and inter-object relationships. Specifically, Scene-Bench consists of a large-scale dataset of scene graphs, and an autonomous evaluation pipeline. The overview of Scene-Bench is shown in Fig. 2.

### 3.1. MegaSG: a large-scale dataset of scene graphs

**Creation of the Dataset.** Due to the complexity and high cost of manual annotation, existing scene graph datasets, such as Visual Genome [31], are relatively small in scale (*e.g.*, only 5k images are prepared for the test set [27]). The limited size and inherent long-tail distribution make these datasets inadequate for studying diffusion models across diverse scene scenarios. To address this limitation and build a large-scale scene graph dataset, we leverage the reasoning capabilities of multimodal large language models (LLMs) in combination with pre-existing object detection datasets. Specifically, we collect 1 million images from COCO [9], Object365 [55], and Open Images v6 [32], which offer rich object categories and bounding boxes. These datasets are ideal for generating large-scale scene graphs efficiently. For additional details, please see Appendix A of the SMs<sup>1</sup>.

**Dataset Quality.** To quantitatively verify the quality of MegaSG, we evaluate state-of-the-art Scene Graph Generation (SGG) models trained on different datasets. For instance, the OvSGTR (Swin-B) [11] model trained on MegaSG achieves a zero-shot performance recall of 45.71% (R@50, PredCls mode) on the VG150 test set, outperforming models trained on smaller datasets like COCO Caption

<sup>1</sup>Through this paper, SMs refers to supplementary materials.

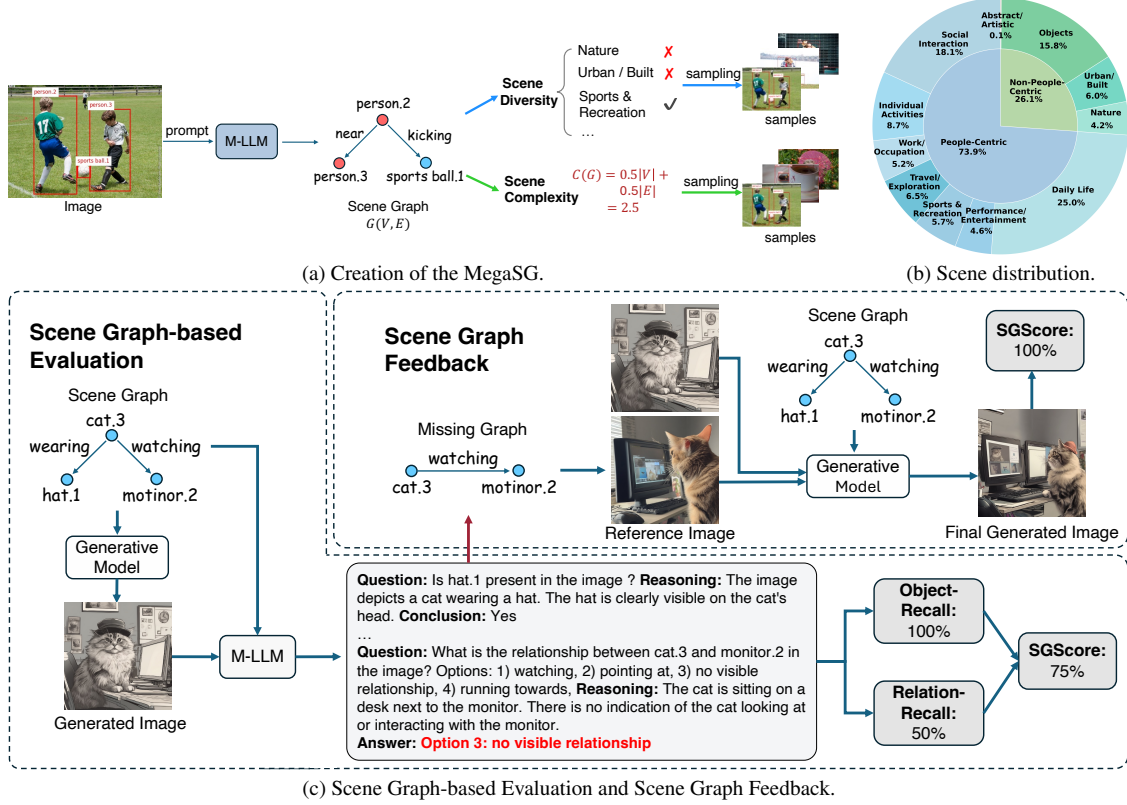


Figure 2. Overview of the Scene-Bench. (a) Scene graphs are generated from images using a multimodal LLM (M-LLM), capturing object relationships and interactions. Scene Diversity and Scene Complexity guide sampling to ensure dataset balance. (b) Scene distribution across categories highlights the diversity in People-Centric and Non-People-Centric themes. (c) Scene graph-based evaluation and feedback leverages the M-LLM to calculate object and relationship recall, generating an SGScore metric that quantifies factual consistency between the generated image and the intended scene. The feedback identifies and corrects discrepancies, iteratively refining the generated image.

data (see Tab. 5 of SMs). This improvement reflects the high-quality scene graph annotations of MegaSG, enabling further exploration of training SGG models on MegaSG or generating images from scene graphs on MegaSG.

**Scene Diversity.** To better understand the behavior of diffusion models in diverse scene scenarios, we utilized an LLM (e.g., Gemini 1.5 Flash [51]) to classify the MegaSG dataset into two main themes: *People-Centric* and *Non-People-Centric*. The *People-Centric* theme includes fine-grained categories such as *Social Interaction*, *Individual Activities*, *Work / Occupation*, *Travel / Exploration*, *Sports & Recreation*, *Performance / Entertainment*, *Daily Life*. For the *Non-people-Centric* theme, we identified categories like *Nature*, *Urban / Built*, *Objects*, and *Abstract / Artistic*. The hierarchical distribution of these categories is illustrated in Fig. 2 (b). And samples are shown in the figure (see Fig. 5 of SMs), showcasing the diversity and range of scenarios covered in the dataset.

**Scene Complexity.** In addition to categorizing natural scenes, measuring scene complexity is crucial for evaluating the performance of diffusion models. While simple

scenes are generally easier for these models to handle, complex scenes pose greater challenges. This raises an important question: *How can we quantitatively define the complexity of a natural scene?*

In this work, we define the complexity of a scene based on its scene graph  $G = (V, E)$ , where  $V$  represents the set of nodes (objects) and  $E$  represents the set of edges (relationships). The complexity is calculated as

$$C(G) = \gamma \cdot |V| + (1.0 - \gamma) \cdot |E|, \quad (1)$$

where  $\gamma \in [0, 1]$  is a weighting factor that balances the influence of the number of nodes and edges.

The scene graph representation provides a straightforward way to quantify complexity, making it possible to analyze the performance of diffusion models across a range of difficulty levels, from simple to highly complex scenes. In contrast, defining the complexity of a text prompt is inherently more challenging due to the lack of explicit structural information. By leveraging this graph-based approach, we can better understand how diffusion models respond to varying levels of scene complexity, offering insights into



their strengths and limitations across different scenarios.

**Dataset Comparison.** We compare the MegaSG with existing scene graph datasets, specifically Visual Genome (VG) [31] and COCO-Stuff [6], as summarized in Tab. 1. MegaSG significantly outperforms VG and COCO-Stuff in terms of scale, encompassing 1 million images compared to VG’s 108k and COCO-Stuff’s 4.5k. Additionally, MegaSG offers a substantially richer vocabulary with 775 object categories and 122 relations, enhancing the diversity and complexity of scene annotations. Importantly, MegaSG’s test set is *complexity balanced*, ensuring an even distribution of simple, medium, and hard scenes, whereas VG and COCO-Stuff lack this balanced composition.

### 3.2. Evaluation Strategy

To quantify the factual consistency, we utilize a multimodal LLM (M-LLM) to assess the recall of objects and relationships, as shown in Fig. 2 (c).

**Recall of Objects.** Given a generated image  $I$  and its intended scene graph  $G = (V, E)$ , where  $V$  represents the set of objects (nodes) and  $E$  represents the relationships (edges), we prompt the M-LLM with specific queries about the existence of each object. For example, for a scene graph containing the relationships:  $\{“source”: “person.2”, “target”: “sports ball.1”, “relation”: “kicking”\}$ ,  $\{“source”: “person.2”, “target”: “person.3”, “relation”: “near”\}$ , we would prompt the M-LLM with questions such as “Is there a sports ball in the image?”. The M-LLM, based on its multimodal capabilities, examines the generated image and responds with a binary answer (Yes / No) to indicate whether the specified object is present. We define the object recall as the fraction of correctly identified objects in the generated image:

$$\text{ObjectRecall}(G, I) = \frac{|V_{\text{pred}} \cap V_{\text{gt}}|}{|V_{\text{gt}}|}, \quad (2)$$

where  $V_{\text{pred}}$  is the set of objects the LLM identifies as present in the image, and  $V_{\text{gt}}$  is the set of ground-truth objects from the original scene graph.

**Recall of Relationships.** To further assess the quality of the generated scene, we evaluate the recall of relationships between objects in the image. For each relationship  $r \in E$ , we check whether the predicted relationship  $r_{\text{pred}}$  exists between the corresponding objects in the generated image. The relationship recall is defined as:

$$\text{RelationRecall}(G, I) = \frac{|E_{\text{pred}} \cap E_{\text{gt}}|}{|E_{\text{gt}}|}, \quad (3)$$

where  $E_{\text{pred}}$  represents the predicted relationships between objects in the generated scene, and  $E_{\text{gt}}$  represents the ground-truth relationships from the original scene graph. To obtain  $E_{\text{pred}}$ , we prompt the LLM with multiple-choice

questions such as: “What is the relationship between the person and the sports ball in the image? A) kicking; B) throwing; C) holding; D) no visible relationship.”

**SGScore.** In addition to individual recalls of objects and relationships, we introduce a comprehensive metric, *SGScore*, which evaluates the overall quality of the scene graph in terms of both objects and relationships. *SGScore* is computed as a weighted combination of object recall and relationship recall:

$$\text{SGScore}(G, I) = \alpha \cdot \text{ObjectRecall}(G, I) + (1.0 - \alpha) \cdot \text{RelationRecall}(G, I), \quad (4)$$

where  $\alpha \in [0, 1]$  is a hyperparameter that controls the relative importance of object recall versus relationship recall. By adjusting this weight, we can tune the evaluation to place more emphasis on either the objects or the relationships, depending on the task requirements. *SGScore* provides a holistic evaluation of how well the generated scene aligns with the scene graph, offering a balanced measure that reflects both object accuracy and relationship consistency.

## 4. Scene Graph Feedback

Building on the scene graph-based evaluation, we propose a scene graph feedback to iteratively refine the generated image based on identified discrepancies between the image and the input scene graph. This process leverages multimodal LLMs to analyze the generated scene and provide targeted feedback for refinement.

Specifically, given a scene graph  $G = (V, E)$ , we first perform scene composition using an LLM (see Tab. 6 in the SMs), in which nodes and edges are seamlessly integrated into a *prompt* for an exact scene. This *prompt* results in an initial image  $I_0$  through the diffusion model  $f_D$ . With the input scene graph  $G$  and the generated image  $I_0$ , a multimodal LLM  $f_M$  has been applied to evaluate the presence of objects and relationships. The missing objects and relationships are constructed as a missing graph  $G_{\text{miss}}$ . If discrepancies exist, e.g.,  $G_{\text{miss}} \neq (\emptyset, \emptyset)$ , we will generate a reference image  $I_1$  conditioned on the  $G_{\text{miss}}$  as does in generating  $I_0$  conditioned on  $G$ . To generate the final output image, we use IP-Adapter [68] to integrate *prompt*,  $I_0$ , and  $I_1$ , in which the cross attention process can be formulated as

$$\begin{aligned} Z = & \text{Attention}(Q, K_{\text{prompt}}, V_{\text{prompt}}) + \\ & \lambda_0 \cdot \text{Attention}(Q, K_{I_0}, V_{I_0}) + \\ & \lambda_1 \cdot \text{Attention}(Q, K_{I_1}, V_{I_1}), \end{aligned} \quad (5)$$

where  $Q$  is the query features of the latent variable,  $K_{\text{prompt}} / V_{\text{prompt}}$ ,  $K_{I_0} / V_{I_0}$ ,  $K_{I_1} / V_{I_1}$ , are the projected features of *prompt*,  $I_0$ ,  $I_1$ , respectively. The Attention is defined as  $\text{Attention}(Q, K, V) = \text{softmax}(\frac{QK^T}{\sqrt{d}})V$  as does in [59].  $\lambda_0, \lambda_1$  are weight factors.

## 5. Experiments

### 5.1. Experimental Setup

**Models.** We evaluate several popular diffusion models on Scene-Bench, including variants of Stable Diffusion and other state-of-the-art methods.

**Datasets.** We use the Visual Genome dataset [31] following the data splits from SG2Im [27], and the proposed MegaSG dataset. For a fair comparison, we balance samples for testing based on Scene Diversity and Scene Complexity (see SMs).

**Metrics.** We employ common metrics such as Inception Score (IS) [53], Fr chet Inception Distance (FID) [22], and CLIPScore [21]. Additionally, we introduce ObjectRecall, RelationRecall, and SGScore (see Sec. 3.2 and Appendix B.1 of the SMs for details).

**Scene Graph Representation.** For text-to-image (T2I) models that condition on a sentence, we encode scene graphs in the format “{subject} {predicate} {object}” (e.g., cat sitting on desk, dog near chair). For the prompt that converts a scene graph into a consistent description (i.e., scene composition in Sec. 4), please refer to Appendix B.1 of the SMs.

**Scene Complexity.** Based on Scene complexity defined as Eq. (1), we categorize the scene complexity into three levels: *simple*, *medium*, and *hard* (details in Appendix B.1 of the SMs).

**LLM.** We use Gemini 1.5 Flash [51] (cutoff November 2024) as the multimodal LLM in our experiments. We also report results using local multimodal LLMs like LLaVA [39] in Appendix C.1 of the SMs.

### 5.2. Evaluation of Scene-Bench

**Performance on Visual Genome.** Table 2 presents the results on the VG test set. The first finding is that *SGScore* provides much more distinguishability than other metrics like FID and CLIPScore. For instance, SD v1.5 has a better FID score than SD v2.1 (42.8 vs. 46.6), yet its *SGScore* is lower than that of SD v2.1 (52.5 vs. 54.4), indicating there are more missed objects and relationships in the images generated by SD v1.5. Another finding is that due to the VG test set being biased towards simple scenes, the performance on medium and hard scenes is counterintuitive: the performance should decrease as scene complexity increases, but this trend is not consistently observed, largely because of the limited number of complex scenes in the test set. This counterexample justifies why we need a new large-scale benchmark to evaluate models comprehensively.

**Performance on MegaSG.** To fairly assess models’ abilities to handle more complex scenes, we evaluated them on a large-scale subset of the MegaSG dataset, sampled by Scene Complexity ( $\gamma = 0$ ). As shown in Tab. 3, we observe a general decline in performance across all models. For example,

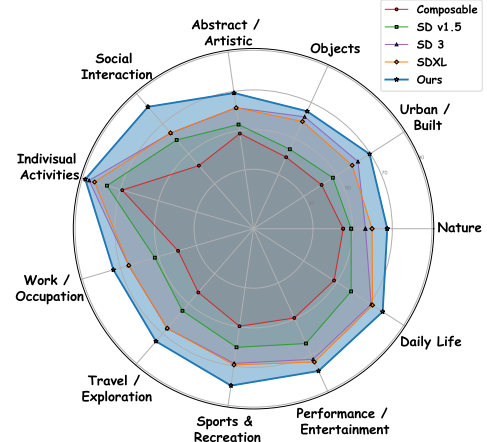


Figure 3. Comparison of model performances using *SGScore* across various scene categories.

SD v1.5’s *SGScore* drops from 64.9 (simple scenes) to 44.7 (hard scenes), indicating they struggle more with accurately modeling the relationships in complex scenes.

**Performance Across Scene Diversity.** We evaluated model performance across diverse scene categories identified in our Scene Diversity analysis (see Section 3.1). Fig. 3 presents results for categories like *Social Interaction*, *Nature*, and *Urban Environments*. Models generally perform better in categories like *Individual Activities*, *Performance / Entertainment*, and *Daily Life*, but face challenges in *Social Interaction* (where scenes often include multiple people) and *Abstract / Artistic* (due to style discrepancies), etc. This variation underscores the importance of evaluating models across a broad range of scenarios to comprehensively assess their strengths and limitations.

**Impact of Scene Complexity.** Beyond the three coarse levels, we evaluate model performance across a complexity range from 1 to 10. Detailed experimental results and analysis are provided in Section B.2 of the SMs. Our findings reveal that, although image quality (measured by FID) remains stable, increasing scene complexity significantly degrades the factual consistency of scene representations (measured by *SGScore*). Notably, our model consistently outperforms competitors by maintaining higher object and relationship recall across all complexity levels.

### 5.3. Evaluation of Scene Graph Feedback

We evaluated our scene graph feedback pipeline using two diffusion models: SD v1.5 [52] and SDXL [48]. For each model, we compared three settings: baseline (without scene composition or feedback), with scene composition only, and with both scene composition and feedback.

**Results and Analysis.** Table 4 summarizes the results. For SD v1.5, the baseline achieved an ObjectRecall of 64.93% and a RelationRecall of 44.19% (*SGScore* 54.56%). In-

Method	Resolution	IS $\uparrow$	FID $\downarrow$	CLIPScore $\uparrow$	SGScore $\uparrow$			
					Overall	Simple (# 3993)	Medium (# 930)	Hard (# 173)
SGDiff [66]	256x256	16.0	29.6	-	64.5	64.2	66.3	61.5
SceneGenie [16]	256x256	20.2	42.2	-	-	-	-	-
Composable [42]	512x512	20.5	47.5	22.0	48.0	48.9	45.0	44.5
Structured [17]	512x512	23.0	42.2	22.0	52.5	51.8	54.6	56.1
SD v1.5 [52]	512x512	23.1	42.8	22.0	52.5	51.9	54.7	53.9
SD v2.1 [52]	768x768	20.8	46.6	22.1	54.4	53.5	57.8	57.9
PixArt- $\alpha$ [8]	1024x1024	20.8	52.9	22.1	59.8	58.5	64.1	67.0
SD3.5 [14]	1024x1024	21.5	45.6	22.1	60.5	59.4	64.1	65.9
SD3 [14]	1024x1024	23.4	44.5	22.1	62.1	60.9	66.3	66.7
SDXL [48]	1024x1024	23.1	43.4	22.1	60.7	59.6	64.0	69.6
RPG [67] (SDXL)	1024x1024	22.9	44.2	19.3	69.3 (+14.2%)	69.4 (+16.4%)	68.7 (+7.3%)	70.5 (+1.3%)
Ours (SD v1.5)	512x512	20.7	41.6	19.1	65.1 (+24.0%)	65.1 (+25.4%)	65.1 (+19.0%)	66.8 (+23.9%)
Ours (SDXL)	1024x1024	21.0	42.7	19.3	74.1 (+22.1%)	74.2 (+24.5%)	73.3 (+14.5%)	75.3 (+8.2%)

Table 2. Model Comparison on the VG test set. Models including SGDiff and SceneGenie are trained on VG train set. Since SceneGenie [16] does not release the code, we only present the reported IS and FID.

Method	Resolution	IS $\uparrow$	FID $\downarrow$	CLIPScore $\uparrow$	SGScore $\uparrow$			
					Overall	Simple (# 15k)	Medium (# 20k)	Hard (# 15k)
Composable [42]	512x512	20.3	41.0	22.9	42.0	61.0	39.0	28.3
Structured [17]	512x512	28.6	26.2	23.0	53.9	65.1	53.9	46.0
SD v1.5 [52]	512x512	27.0	29.1	22.8	54.2	64.9	53.4	44.7
SD v2.1 [52]	768x768	24.9	34.0	22.9	57.8	68.2	56.4	49.2
PixArt- $\alpha$ [8]	1024x1024	24.3	43.9	23.0	59.5	68.4	58.2	52.7
SD3.5 [14]	1024x1024	25.9	34.5	23.0	63.4	73.1	61.9	55.7
SD3 [14]	1024x1024	27.2	35.5	23.0	65.2	74.2	63.8	58.0
SDXL [48]	1024x1024	25.3	31.6	23.0	65.6	72.9	64.6	59.6
RPG [67] (SDXL)	1024x1024	23.4	37.5	20.0	71.0 (+8.2%)	76.5 (+4.9%)	70.5 (+9.1%)	66.1 (+10.9%)
Ours (SD v1.5)	512x512	23.1	28.9	19.9	62.0 (+14.4%)	71.0 (+9.4%)	61.3 (+14.8%)	53.9 (+20.6%)
Ours (SDXL)	1024x1024	21.6	34.1	20.0	77.1 (+17.5%)	81.8 (+12.2%)	76.6 (+18.6%)	73.1 (+22.7%)

Table 3. Model comparison on a 50,000-image subset of the MegaSG dataset, sampled with a Scene Complexity of  $\gamma = 0$ . Scene graph-based methods such as SGDiff [66], which are limited by the vocabulary of the VG dataset, were excluded from testing.

incorporating scene composition improved these metrics to 75.45% and 48.84% (SGScore 62.14%), demonstrating that detailed prompts help the model better capture specified objects and relationships. Applying our feedback strategy further increased ObjectRecall to 79.93% and RelationRecall to 53.97% (SGScore 66.95%), indicating effective correction of discrepancies. A similar trend was observed in SDXL, where improvements after applying scene composition and feedback increased the SGScore from 65.50% to 77.25%.

Compared with LLM-based methods like RPG [67], the performance gain on VG or MegaSG is significant. RPG [67] utilizes an LLM as an agent to perform recaptioning, region planning and merging, while it lacks a feedback for ensuring factual consistency.

These results demonstrate that our scene graph feedback effectively enhances factual consistency by identifying and correcting discrepancies between generated images and the intended scene graphs.

**Ablation Study of IP-Adapter.** To assess the impact of the additional parameters introduced by the IP-Adapter, we conduct an ablation study. Detailed results are provided in

Model	ObjectRecall $\uparrow$	RelationRecall $\uparrow$	SGScore $\uparrow$
SD v1.5 [52]			
Baseline	64.93 $\pm$ 0.31	44.19 $\pm$ 0.09	54.56 $\pm$ 0.12
+ Scene Composition	75.45 $\pm$ 0.19	48.84 $\pm$ 0.39	62.14 $\pm$ 0.25
+ Feedback	<b>79.93 <math>\pm</math> 0.34</b>	<b>53.97 <math>\pm</math> 0.20</b>	<b>66.95 <math>\pm</math> 0.23</b>
SDXL [48]			
Baseline	77.22 $\pm$ 0.22	53.78 $\pm$ 0.36	65.50 $\pm$ 0.19
+ Scene Composition	88.07 $\pm$ 0.17	60.37 $\pm$ 0.14	74.22 $\pm$ 0.14
+ Feedback	<b>91.30 <math>\pm</math> 0.24</b>	<b>63.20 <math>\pm</math> 0.10</b>	<b>77.25 <math>\pm</math> 0.21</b>

Table 4. Effectiveness of the scene graph feedback on 5,000 images sampled from MegaSG.

Appendix B.3 of the SMs.

## 5.4. Qualitative Evaluation

We present qualitative results to demonstrate the effectiveness of Scene-Bench and the proposed scene graph feedback. Fig. 4 compares images generated by various models using the same scene graphs. Most of models often struggle with complex scenes, leading to images with missing objects or incorrectly depicted relationships. For example, when generating a scene from the scene graph



Figure 4. Comparison of Scene Graph-based Image Generation across Different Models. Each row displays a unique scene graph used as input for image generation. We present the **SGScore** below each generated image to quantify the consistency between the scene graph and the generated output.

$\langle \text{person.2, holding, baseball glove.1} \rangle$ ,  $\langle \text{person.3, wearing, helmet.4} \rangle$ , previous models may omit the *helmet* or fail to represent *person wearing helmet*.

With the proposed scene graph feedback, the generated image more faithfully represents the intended scene graph. The feedback process identifies missing elements and corrects relational inaccuracies, resulting in the image where one person is wearing a helmet and another is holding a baseball glove. This demonstrates the model’s improved ability to handle complex object interactions and spatial arrangements, highlighting the benefits of our approach.

## 5.5. Human Evaluation

To validate the efficacy of *SGScore* in improving the verification of factual consistency and assess the impact of the proposed feedback pipeline, we conducted a human evaluation. Annotators were presented with 1,000 four-to-one comparative queries (see examples in Appendix B.4 of the SMs). Each query displayed an original image alongside four generated images produced by different models. Annotators were instructed to select the image that most accurately preserved the object presence and relationships of the original. As illustrated in Fig. 9 of the SMs, both human judgments and machine-based selections consistently favored our model, thereby confirming its superior factual consistency as measured by *SGScore*.

## 6. Discussion

In the field of SG2IM, most existing approaches [3, 16, 27, 40, 56, 62, 66] focus primarily on network architecture design, train on widely used datasets (*e.g.*, Visual Genome and COCO-stuff), and report conventional metrics such as

IS, FID, and CLIPScore. However, *assessing factual consistency and leveraging identified inconsistency as feedback remain underexplored*. To address this gap, we introduce a large-scale scene graph dataset, a novel metric *SGScore*, and an automatic evaluation pipeline to systematically measure the factual consistency in SG2IM. Based on the evaluation pipeline, we incorporate a training-free feedback pipeline to enhance factual consistency.

One potential concern for the newly introduced dataset, *MegaSG*, is its lack of attribute annotations (*e.g.*, color, shape, texture) that are present in the VG dataset. To assess the impact of this omission, we present an experimental analysis in Appendix D.2 of the SMs. The results indicate that explicit attribute binding yields a marginal difference. Considering the trade-off between additional annotation costs and minimal gains, we opted to omit attributes in the construction of *MegaSG*. Beyond this concern, we compare *Scene-Bench* with existing T2I benchmarks like TIFA [24] and DSG [12] in Appendix D.3 to validate the reliability of *SGScore*.

## 7. Conclusion

In this work, we introduce *Scene-Bench*, a comprehensive benchmark for evaluating the factual consistency of generating natural scenes from scene graphs. Our benchmark incorporates a large-scale dataset, *MegaSG*, with a novel metric, *SGScore*, which quantitatively assesses both the presence of objects and the accuracy of relationships through the reasoning capabilities of multimodal LLMs. Building upon this evaluation, our scene graph feedback mechanism iteratively refines generated images by correcting inconsistencies between the scene graph and the output.



This process significantly improves the factual consistency. Extensive experiments demonstrate that *Scene-Bench* offers a rigorous evaluation framework, especially in complex scenes where traditional metrics fall short. We believe that *Scene-Bench* will establish a new standard and inspire future research in high-fidelity, controllable generation.

## References

- [1] Josh Achiam, Steven Adler, Sandhini Agarwal, Lama Ahmad, Ilge Akkaya, Florencia Leoni Aleman, Diogo Almeida, Janko Altenschmidt, Sam Altman, Shyamal Anadkat, et al. GPT-4 technical report. *arXiv preprint arXiv:2303.08774*, 2023. 4, 5
- [2] Google AI. Gemini 1.5 flash pricing. [https://ai.google.dev/pricing#1\\_5flash](https://ai.google.dev/pricing#1_5flash), 2024. 6, 9
- [3] Oron Ashual and Lior Wolf. Specifying object attributes and relations in interactive scene generation. In *ICCV*, pages 4561–4569, 2019. 3, 8
- [4] Andrew Brock, Jeff Donahue, and Karen Simonyan. Large scale GAN training for high fidelity natural image synthesis. In *ICLR*, 2019. 1
- [5] Tom Brown, Benjamin Mann, Nick Ryder, Melanie Subbiah, Jared D Kaplan, Prafulla Dhariwal, Arvind Neelakantan, Pranav Shyam, Girish Sastry, Amanda Askell, et al. Language models are few-shot learners. *NeurIPS*, 33:1877–1901, 2020. 8
- [6] Holger Caesar, Jasper Uijlings, and Vittorio Ferrari. Coco-stuff: Thing and stuff classes in context. In *CVPR*, pages 1209–1218, 2018. 2, 3, 5
- [7] Agneet Chatterjee, Gabriela Ben Melech Stan, Estelle Aflalo, Sayak Paul, Dhruva Ghosh, Tejas Gokhale, Ludwig Schmidt, Hannaneh Hajishirzi, Vasudev Lal, Chitta Baral, and Yezhou Yang. Getting it right: Improving spatial consistency in text-to-image models. In *ECCV*, pages 204–222, 2024. 1, 2, 3
- [8] Junsong Chen, Jincheng Yu, Chongjian Ge, Lewei Yao, Enze Xie, Zhongdao Wang, James T. Kwok, Ping Luo, Huchuan Lu, and Zhenguo Li. PixArt- $\alpha$ : Fast training of diffusion transformer for photorealistic text-to-image synthesis. In *ICLR*, 2024. 7, 3
- [9] Xinlei Chen, Hao Fang, Tsung-Yi Lin, Ramakrishna Vedantam, Saurabh Gupta, Piotr Dollár, and C. Lawrence Zitnick. Microsoft COCO captions: Data collection and evaluation server. *CoRR*, abs/1504.00325, 2015. 3, 1
- [10] Yen-Chun Chen, Linjie Li, Licheng Yu, Ahmed El Kholy, Faisal Ahmed, Zhe Gan, Yu Cheng, and Jingjing Liu. UNITER: universal image-text representation learning. In *ECCV*, pages 104–120, 2020. 3
- [11] Zuyao Chen, Jinlin Wu, Zhen Lei, Zhaoxiang Zhang, and Changwen Chen. Expanding scene graph boundaries: Fully open-vocabulary scene graph generation via visual-concept alignment and retention. In *ECCV*, 2024. 2, 3, 1
- [12] Jaemin Cho, Yushi Hu, Jason M. Baldridge, Roopal Garg, Peter Anderson, Ranjay Krishna, Mohit Bansal, Jordi Pont-Tuset, and Su Wang. Davidsonian scene graph: Improving reliability in fine-grained evaluation for text-to-image generation. In *ICLR*, 2024. 8, 9
- [13] Kevin Clark and Priyank Jaini. Text-to-image diffusion models are zero shot classifiers. *NeurIPS*, 36:58921–58937, 2023. 7
- [14] Patrick Esser, Sumith Kulal, Andreas Blattmann, Rahim Entezari, Jonas Müller, Harry Saini, Yam Levi, Dominik Lorenz, Axel Sauer, Frederic Boesel, et al. Scaling rectified flow transformers for high-resolution image synthesis. In *ICML*, 2024. 1, 7, 3
- [15] Ying Fan, Olivia Watkins, Yuqing Du, Hao Liu, Moonkyung Ryu, Craig Boutilier, Pieter Abbeel, Mohammad Ghavamzadeh, Kangwook Lee, and Kimin Lee. Reinforcement learning for fine-tuning text-to-image diffusion models. *NeurIPS*, 2024. 1
- [16] Azade Farshad, Yousef Yeganeh, Yu Chi, Chengzhi Shen, Björn Ommer, and Nassir Navab. Scenegenie: Scene graph guided diffusion models for image synthesis. In *ICCVW*, pages 88–98, 2023. 3, 7, 8
- [17] Weixi Feng, Xuehai He, Tsu-Jui Fu, Varun Jampani, Arjun R. Akula, Pradyumna Narayana, Sugato Basu, Xin Eric Wang, and William Yang Wang. Training-free structured diffusion guidance for compositional text-to-image synthesis. In *ICLR*, 2023. 1, 3, 7
- [18] Weixi Feng, Wanrong Zhu, Tsu-jui Fu, Varun Jampani, Arjun Akula, Xuehai He, Sugato Basu, Xin Eric Wang, and William Yang Wang. Layoutgpt: Compositional visual planning and generation with large language models. *NeurIPS*, 2024. 3
- [19] Ian Goodfellow, Jean Pouget-Abadie, Mehdi Mirza, Bing Xu, David Warde-Farley, Sherjil Ozair, Aaron Courville, and Yoshua Bengio. Generative adversarial nets. In *NeurIPS*, pages 2672–2680, 2014. 1
- [20] Ian Goodfellow, Jean Pouget-Abadie, Mehdi Mirza, Bing Xu, David Warde-Farley, Sherjil Ozair, Aaron Courville, and Yoshua Bengio. Generative adversarial networks. *Communications of the ACM*, 63(11):139–144, 2020. 3
- [21] Jack Hessel, Ari Holtzman, Maxwell Forbes, Ronan Le Bras, and Yejin Choi. CLIPScore: A reference-free evaluation metric for image captioning. In *EMNLP*, pages 7514–7528, 2021. 1, 2, 6, 3
- [22] Martin Heusel, Hubert Ramsauer, Thomas Unterthiner, Bernhard Nessler, and Sepp Hochreiter. Gans trained by a two time-scale update rule converge to a local nash equilibrium. *NeurIPS*, 2017. 2, 6, 3
- [23] Jonathan Ho, Ajay Jain, and Pieter Abbeel. Denoising diffusion probabilistic models. *NeurIPS*, 33:6840–6851, 2020. 1
- [24] Yushi Hu, Benlin Liu, Jungo Kasai, Yizhong Wang, Mari Ostendorf, Ranjay Krishna, and Noah A Smith. Tifa: Accurate and interpretable text-to-image faithfulness evaluation with question answering. In *ICCV*, pages 20406–20417, 2023. 8
- [25] Phillip Isola, Jun-Yan Zhu, Tinghui Zhou, and Alexei A Efros. Image-to-image translation with conditional adversarial networks. In *CVPR*, pages 1125–1134, 2017. 1
- [26] Justin Johnson, Ranjay Krishna, Michael Stark, Li-Jia Li, David Shamma, Michael Bernstein, and Li Fei-Fei. Image

- retrieval using scene graphs. In *CVPR*, pages 3668–3678, 2015. 2
- [27] Justin Johnson, Agrim Gupta, and Li Fei-Fei. Image generation from scene graphs. In *CVPR*, pages 1219–1228, 2018. 3, 6, 8, 7
- [28] Tero Karras, Samuli Laine, and Timo Aila. A style-based generator architecture for generative adversarial networks. In *CVPR*, pages 4401–4410, 2019. 1
- [29] Bahjat Kawar, Shiran Zada, Oran Lang, Omer Tov, Huiwen Chang, Tali Dekel, Inbar Mosseri, and Michal Irani. Imagic: Text-based real image editing with diffusion models. In *CVPR*, pages 6007–6017, 2023. 1
- [30] Diederik P. Kingma and Max Welling. Auto-encoding variational bayes. In *ICLR*, 2014. 1
- [31] Ranjay Krishna, Yuke Zhu, Oliver Groth, Justin Johnson, Kenji Hata, Joshua Kravitz, Stephanie Chen, Yannis Kalantidis, Li-Jia Li, David A Shamma, et al. Visual genome: Connecting language and vision using crowdsourced dense image annotations. *IJCV*, 123:32–73, 2017. 2, 3, 5, 6
- [32] Alina Kuznetsova, Hassan Rom, Neil Alldrin, Jasper Uijlings, Ivan Krasin, Jordi Pont-Tuset, Shahab Kamali, Stefan Popov, Matteo Mallocci, Alexander Kolesnikov, et al. The open images dataset v4: Unified image classification, object detection, and visual relationship detection at scale. *IJCV*, 128(7):1956–1981, 2020. 3, 1
- [33] Kimin Lee, Hao Liu, Moonkyung Ryu, Olivia Watkins, Yuqing Du, Craig Boutilier, Pieter Abbeel, Mohammad Ghavamzadeh, and Shixiang Shane Gu. Aligning text-to-image models using human feedback. *CoRR*, abs/2302.12192, 2023. 1
- [34] Chenliang Li, Haiyang Xu, Junfeng Tian, Wei Wang, Ming Yan, Bin Bi, Jiabo Ye, He Chen, Guohai Xu, Zheng Cao, Ji Zhang, Songfang Huang, Fei Huang, Jingren Zhou, and Luo Si. mplug: Effective and efficient vision-language learning by cross-modal skip-connections. In *EMNLP*, pages 7241–7259, 2022. 8
- [35] Junnan Li, Dongxu Li, Silvio Savarese, and Steven Hoi. Blip-2: Bootstrapping language-image pre-training with frozen image encoders and large language models. In *ICML*, pages 19730–19742, 2023. 2
- [36] Junnan Li, Dongxu Li, Silvio Savarese, and Steven C. H. Hoi. BLIP-2: bootstrapping language-image pre-training with frozen image encoders and large language models. In *ICML*, pages 19730–19742, 2023. 8
- [37] Long Lian, Boyi Li, Adam Yala, and Trevor Darrell. Llm-grounded diffusion: Enhancing prompt understanding of text-to-image diffusion models with large language models. *arXiv preprint arXiv:2305.13655*, 2023. 3
- [38] Haotian Liu, Chunyuan Li, Yuheng Li, Bo Li, Yuanhan Zhang, Sheng Shen, and Yong Jae Lee. Llava-next: Improved reasoning, ocr, and world knowledge, 2024. 4, 5
- [39] Haotian Liu, Chunyuan Li, Qingyang Wu, and Yong Jae Lee. Visual instruction tuning. *NeurIPS*, 2024. 6
- [40] Jinxiu Liu and Qi Liu. R3CD: Scene graph to image generation with relation-aware compositional contrastive control diffusion. In *AAAI*, pages 3657–3665, 2024. 3, 8, 7
- [41] Minghao Liu, Le Zhang, Yingjie Tian, Xiaochao Qu, Luoqi Liu, and Ting Liu. Draw like an artist: Complex scene generation with diffusion model via composition, painting, and retouching. *arXiv preprint arXiv:2408.13858*, 2024. 1, 3
- [42] Nan Liu, Shuang Li, Yilun Du, Antonio Torralba, and Joshua B Tenenbaum. Compositional visual generation with composable diffusion models. In *ECCV*, pages 423–439, 2022. 1, 3, 7
- [43] Shilin Lu, Yanzhu Liu, and Adams Wai-Kin Kong. Tf-icon: Diffusion-based training-free cross-domain image composition. In *ICCV*, pages 2294–2305, 2023. 1
- [44] Jiayuan Mao. Scene graph parser. <https://github.com/vacancy/SceneGraphParser>, 2022. 2, 3
- [45] Alex Nichol, Prafulla Dhariwal, Aditya Ramesh, Pranav Shyam, Pamela Mishkin, Bob McGrew, Ilya Sutskever, and Mark Chen. Glide: Towards photorealistic image generation and editing with text-guided diffusion models. *arXiv preprint arXiv:2112.10741*, 2021. 1, 3
- [46] OpenAI. Gpt api pricing. <https://openai.com/api/pricing/>, 2025. 9
- [47] Dong Huk Park, Samaneh Azadi, Xihui Liu, Trevor Darrell, and Anna Rohrbach. Benchmark for compositional text-to-image synthesis. In *NeurIPS*, 2021. 3
- [48] Dustin Podell, Zion English, Kyle Lacey, Andreas Blattmann, Tim Dockhorn, Jonas Müller, Joe Penna, and Robin Rombach. SDXL: improving latent diffusion models for high-resolution image synthesis. In *ICLR*, 2024. 1, 6, 7, 3
- [49] Alec Radford, Jong Wook Kim, Chris Hallacy, Aditya Ramesh, Gabriel Goh, Sandhini Agarwal, Girish Sastry, Amanda Askell, Pamela Mishkin, Jack Clark, et al. Learning transferable visual models from natural language supervision. In *ICML*, pages 8748–8763, 2021. 3
- [50] Aditya Ramesh, Mikhail Pavlov, Gabriel Goh, Scott Gray, Chelsea Voss, Alec Radford, Mark Chen, and Ilya Sutskever. Zero-shot text-to-image generation. In *ICML*, pages 8821–8831, 2021. 3
- [51] Machel Reid, Nikolay Savinov, Denis Teplyashin, Dmitry Lepikhin, Timothy Lillicrap, Jean-baptiste Alayrac, Radu Soricut, Angeliki Lazaridou, Orhan Firat, Julian Schrittwieser, et al. Gemini 1.5: Unlocking multimodal understanding across millions of tokens of context. *arXiv preprint arXiv:2403.05530*, 2024. 4, 6, 1, 5
- [52] Robin Rombach, Andreas Blattmann, Dominik Lorenz, Patrick Esser, and Björn Ommer. High-resolution image synthesis with latent diffusion models. In *CVPR*, pages 10684–10695, 2022. 1, 3, 6, 7
- [53] Tim Salimans, Ian Goodfellow, Wojciech Zaremba, Vicki Cheung, Alec Radford, and Xi Chen. Improved techniques for training gans. *NeurIPS*, 29, 2016. 6, 3
- [54] Christoph Schuhmann, Romain Beaumont, Richard Vencu, Cade Gordon, Ross Wightman, Mehdi Cherti, Theo Coombes, Aarush Katta, Clayton Mullis, Mitchell Wortsman, et al. Laion-5b: An open large-scale dataset for training next generation image-text models. *NeurIPS*, 35:25278–25294, 2022. 8
- [55] Shuai Shao, Zeming Li, Tianyuan Zhang, Chao Peng, Gang Yu, Xiangyu Zhang, Jing Li, and Jian Sun. Objects365:

- A large-scale, high-quality dataset for object detection. In *ICCV*, pages 8430–8439, 2019. 3, 1
- [56] Guibao Shen, Luozhou Wang, Jiantao Lin, Wenhao Ge, Chaozhe Zhang, Xin Tao, Yuan Zhang, Pengfei Wan, Zhongyuan Wang, Guangyong Chen, et al. Sg-adapter: Enhancing text-to-image generation with scene graph guidance. *arXiv preprint arXiv:2405.15321*, 2024. 3, 8, 7
- [57] Christian Szegedy, Vincent Vanhoucke, Sergey Ioffe, Jon Shlens, and Zbigniew Wojna. Rethinking the inception architecture for computer vision. In *CVPR*, pages 2818–2826, 2016. 3
- [58] Kaihua Tang, Hanwang Zhang, Baoyuan Wu, Wenhan Luo, and Wei Liu. Learning to compose dynamic tree structures for visual contexts. In *CVPR*, pages 6619–6628, 2019. 2
- [59] Ashish Vaswani, Noam Shazeer, Niki Parmar, Jakob Uszkoreit, Llion Jones, Aidan N. Gomez, Lukasz Kaiser, and Illia Polosukhin. Attention is all you need. In *NeurIPS*, pages 5998–6008, 2017. 5
- [60] Patrick von Platen, Suraj Patil, Anton Lozhkov, Pedro Cuenca, Nathan Lambert, Kashif Rasul, Mishig Davaadorj, Dhruv Nair, Sayak Paul, William Berman, Yiyi Xu, Steven Liu, and Thomas Wolf. Diffusers: State-of-the-art diffusion models. <https://github.com/huggingface/diffusers>, 2022. 3, 4
- [61] Peng Wang, Shuai Bai, Sinan Tan, Shijie Wang, Zhihao Fan, Jinze Bai, Keqin Chen, Xuejing Liu, Jialin Wang, Wenbin Ge, et al. Qwen2-vl: Enhancing vision-language model’s perception of the world at any resolution. *arXiv preprint arXiv:2409.12191*, 2024. 4, 5
- [62] Yunnan Wang, Ziqiang Li, Wenyao Zhang, Zequn Zhang, Baao Xie, Xihui Liu, Wenjun Zeng, and Xin Jin. Scene graph disentanglement and composition for generalizable complex image generation. In *NeurIPS*, 2024. 3, 8
- [63] Tsung-Han Wu, Long Lian, Joseph E Gonzalez, Boyi Li, and Trevor Darrell. Self-correcting llm-controlled diffusion models. In *CVPR*, pages 6327–6336, 2024. 3, 9
- [64] Danfei Xu, Yuke Zhu, Christopher B. Choy, and Li Fei-Fei. Scene graph generation by iterative message passing. In *CVPR*, pages 3097–3106, 2017. 2
- [65] Tao Xu, Pengchuan Zhang, Qiuyuan Huang, Han Zhang, Zhe Gan, Xiaolei Huang, and Xiaodong He. Attngan: Fine-grained text to image generation with attentional generative adversarial networks. In *CVPR*, pages 1316–1324, 2018. 3
- [66] Ling Yang, Zhilin Huang, Yang Song, Shenda Hong, Guohao Li, Wentao Zhang, Bin Cui, Bernard Ghanem, and Ming-Hsuan Yang. Diffusion-based scene graph to image generation with masked contrastive pre-training. *arXiv preprint arXiv:2211.11138*, 2022. 3, 7, 8
- [67] Ling Yang, Zhaochen Yu, Chenlin Meng, Minkai Xu, Stefano Ermon, and CUI Bin. Mastering text-to-image diffusion: Recaptioning, planning, and generating with multi-modal llms. In *ICML*, 2024. 1, 3, 7
- [68] Hu Ye, Jun Zhang, Sibor Liu, Xiao Han, and Wei Yang. IP-Adapter: Text compatible image prompt adapter for text-to-image diffusion models. *CoRR*, abs/2308.06721, 2023. 5
- [69] Keren Ye and Adriana Kovashka. Linguistic structures as weak supervision for visual scene graph generation. In *CVPR*, pages 8289–8299, 2021. 3
- [70] Rowan Zellers, Mark Yatskar, Sam Thomson, and Yejin Choi. Neural motifs: Scene graph parsing with global context. In *CVPR*, pages 5831–5840, 2018. 2, 3
- [71] Han Zhang, Tao Xu, Hongsheng Li, Shaoting Zhang, Xiaogang Wang, Xiaolei Huang, and Dimitris N Metaxas. Stackgan: Text to photo-realistic image synthesis with stacked generative adversarial networks. In *ICCV*, pages 5907–5915, 2017. 3
- [72] Yong Zhang, Yingwei Pan, Ting Yao, Rui Huang, Tao Mei, and Chang Wen Chen. Learning to generate language-supervised and open-vocabulary scene graph using pre-trained visual-semantic space. In *CVPR*, pages 2915–2924, 2023. 1, 3
- [73] Jun-Yan Zhu, Taesung Park, Phillip Isola, and Alexei A Efros. Unpaired image-to-image translation using cycle-consistent adversarial networks. In *ICCV*, pages 2223–2232, 2017. 1

# What Makes a Scene ? Scene Graph-based Evaluation and Feedback for Controllable Generation

## Supplementary Material

### A. MegaSG: a large-scale dataset of scene graphs

**Creation of the Dataset.** We construct the **MegaSG** dataset by leveraging three widely used object detection datasets: COCO [9], Object365 [55], and Open Images v6 [32]. These resources offer diverse scenes with meticulously annotated objects. To ensure the reliability of the scene graphs, we discard images containing fewer than three objects. The annotation prompt used to generate scene graphs from images is detailed in Algorithm 1.

Specifically, the multimodal large language model receives an image—along with associated object categories and bounding boxes—as input and produces a scene graph that depicts the relationships between objects. For example, as illustrated in Fig. 2, the model identifies a “person” kicking a “sports ball” and another “person” nearby, yielding the scene graph: {“source”: “person.2”, “target”: “sports ball.1”, “relation”: “kicking”}, {“source”: “person.2”, “target”: “person.3”, “relation”: “near”}. This structured representation captures both the objects and their spatial as well as relational interactions.

**Scene Diversity.** To classify the scene categories, we utilize an LLM (e.g., Gemini 1.5 Flash [51]) to perform such classification. The prompt used here is *Now, we have a list of image information like {IMAGE\_INFO}, where each image information contains “xyxy” bounding boxes and “relationships” depicting the relation between the “source” object and the “target” object. Please classify the scene in **each image** using the following hierarchy: Level 1: - People-Centric, - Non-People Centric. Level 2: If People-Centric: [Choose one: Social Interaction, Individual Activities, Work/Occupation, Travel/Exploration, Sports & Recreation, Performance/Entertainment, Daily Life]; If Non-People Centric: [Choose one: Nature, Urban/Built, Objects, Abstract/Artistic]. Please provide the classification for each image in the list, and present your answer as a **JSON-formatted** list of dictionaries, where each dictionary corresponds to an image and contains the following keys: “image\_id”, “file\_name”, “level 1”, “level 2”.*

Fig. 5 illustrates examples of categorized scenes in MegaSG, showcasing the diversity and range of scenarios covered in the dataset.

**Dataset Comparison.** To verify the quality of MegaSG, we trained two state-of-the-art SGG models, i.e., VS<sup>3</sup> [72] and OvSGTR [11]. Table 5 reports the zero-shot performance of these two models trained on MegaSG. From the result,

---

#### Algorithm 1 Generate Scene Graph

---

```
import google.generativeai as genai

generation_config = {
    "temperature": 0.7, "top_p": 0.95,
    "top_k": 64, "max_output_tokens": 8192,
    "response_mime_type": "application/json",
}
# Load the generative model
model = genai.GenerativeModel(
    "gemini-1.5-flash",
    generation_config=generation_config
)

prompt_template = """Given a set of detected
objects in an image, each object is
characterized by a name, a bounding box in "(
xmin, ymin, xmax, ymax)" format. Please
generate a scene graph to describe this image.
The scene graph should describe relationships
in the format "source -> relation -> target".
Example Output:\n{"relationships": [{"source":
"object_id1", "target": "object_id2", "relation
":\n"relation_type"}, ... ]}\n Now, objects are
{OBJECTS}. The original width and height of
the provided image are {IMG_WH}. Please output
the scene graph in JSON style without any
comments."""

def annotate(image_name):
    """
    image_name: file path of the image
    """
    # Load image and get its dimensions
    image = Image.open(image_name)
    image_wh = (image.width, image.height)

    # Load objects in the image,
    # e.g., [{"sports ball.1:[312, 360, 370,
    417]", "person.2:[116, 49, 309, 491]", "
    person.3:[367, 108, 550, 477]}]
    image_objects = load_objects(image_name)

    # Construct text prompt
    text_prompt = prompt_template.replace(
        "OBJECTS", str(image_objects)).replace(
        "IMG_WH", str(image_wh))

    # Generate scene graph using generative model
    response = model.generate([
        image, text_prompt])
    return response
```

---

MegaSG significantly improved the performance recall of OvSGTR from 22.79% to 45.71% (R@50, PredCls), offering a strong baseline to scale up SGG models. Beyond the



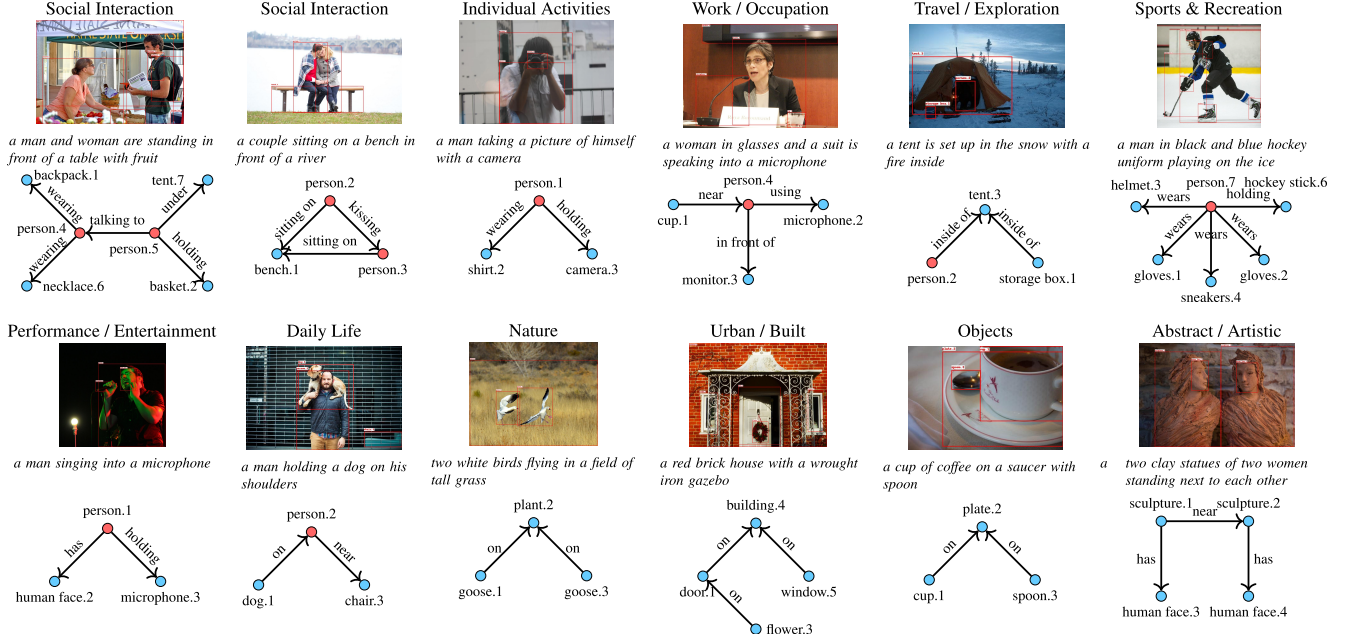


Figure 5. Illustration of scene categories in the MegaSG dataset. The image shows various themes, such as People-Centric (e.g., social interaction, individual activities) and Non-People-Centric (e.g., nature, urban environments). The caption is provided for illustrative purposes and generated using BLIP-2 [35], and the scene graph is constructed as described in Sec. 3.1 and Appendix A.

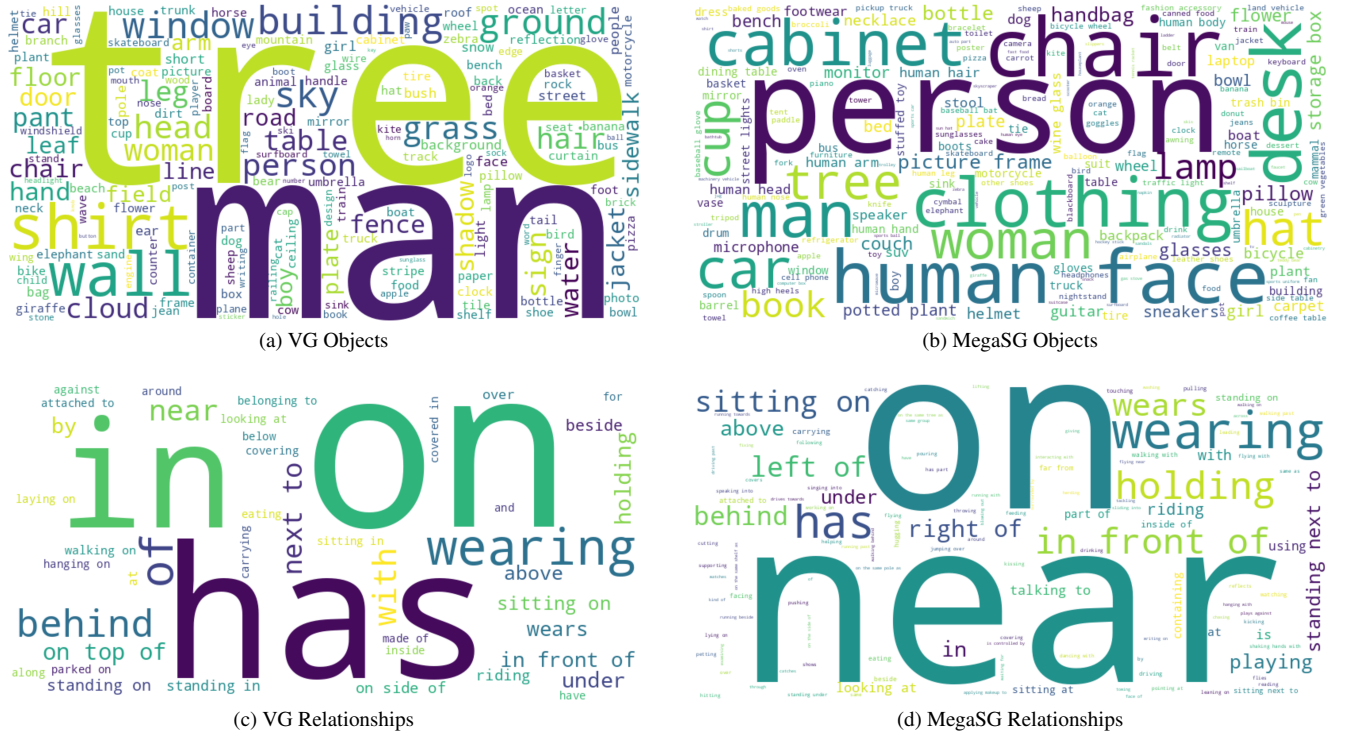


Figure 6. Word clouds of objects and relationships in the Visual Genome (VG) and MegaSG datasets. (a) and (b) illustrate the diversity of objects, while (c) and (d) highlight the relationships. The comparison demonstrates MegaSG’s broader vocabulary and richer representation of object-relationship semantics.

SGG model	Training Data	SGDet						PredCls					
		R@20/50/100			mR@20/50/100			R@20/50/100			mR@20/50/100		
LSWS [69]	COCO [9] Caption (104k)	-	3.28	3.69	-	-	-	-	-	-	-	-	-
MOTIFS [70]		5.02	6.40	7.33	-	-	-	-	-	-	-	-	-
Uniter [10]		5.42	6.74	7.62	-	-	-	-	-	-	-	-	-
VS <sub>(Swin-T)</sub> <sup>3</sup> [72]		4.56	5.79	6.79	2.18	2.59	3.00	12.30	16.77	19.40	3.56	4.79	5.51
VS <sub>(Swin-L)</sub> <sup>3</sup> [72]		4.82	6.20	7.48	2.29	2.70	3.09	12.54	17.28	19.89	3.57	4.83	5.56
OvSGTR <sub>(Swin-T)</sub> [11]		6.61	8.92	10.90	1.09	1.53	1.95	16.65	22.44	26.64	2.47	3.58	4.41
OvSGTR <sub>(Swin-B)</sub> [11]	MegaSG (644k)	6.85	9.33	11.47	1.28	1.79	2.18	16.82	22.79	27.04	2.94	4.24	5.26
VS <sub>(Swin-T)</sub> <sup>3</sup> [72]		5.56	8.19	10.17	1.15	1.71	2.20	23.81	29.64	32.18	4.70	5.96	6.57
VS <sub>(Swin-L)</sub> <sup>3</sup> [72]		9.74	14.80	18.80	1.57	2.71	3.75	31.88	38.77	41.76	5.32	6.88	7.58
OvSGTR <sub>(Swin-T)</sub> [11]		<b>9.94</b>	<b>13.92</b>	<b>17.17</b>	<b>3.05</b>	<b>4.03</b>	<b>4.76</b>	<b>37.12</b>	<b>44.10</b>	<b>47.09</b>	<b>8.49</b>	<b>10.22</b>	<b>11.07</b>
OvSGTR <sub>(Swin-B)</sub> [11]		<b>10.63</b>	<b>14.93</b>	<b>18.36</b>	<b>3.01</b>	<b>4.10</b>	<b>4.99</b>	<b>38.72</b>	<b>45.71</b>	<b>48.51</b>	<b>8.38</b>	<b>10.31</b>	<b>11.07</b>

Table 5. Zero-shot performance of state-of-the-art methods on the VG150 test set. For the COCO Caption dataset, a language parser [44] has been used for extracting triplets from the caption. To prevent information leakage, we sampled 644k images from MegaSG, ensuring that the CLIP similarity of each sampled image with the VG test set remained below 0.9.

SGG task, the vast and diverse scenes offer a valuable resource for training and evaluating diffusion models based on scene graphs.

We compare the word cloud of VG and MegaSG in Fig. 6. From the comparison in the word clouds, both the VG and MegaSG datasets contain similar high-frequency objects like “person”, “tree”, and “man”, as well as common relationships such as “on” and “near”. However, the MegaSG dataset shows a wider variety of object types and relationship terms, suggesting it captures a wider range of visual semantics than the VG dataset.

## B. Experiments

### B.1. Experimental Setup

**Models.** We evaluate several popular open-source diffusion models, including Composable [42], Structured [17], SD v1.5 [52] (checkpoint: *runwayml/stable-diffusion-v1-5*), SD v2.1 [52] (checkpoint: *stabilityai/stable-diffusion-2-1*), PixArt- $\alpha$  [8] (checkpoint: *PixArt-alpha/PixArt-XL-2-1024-MS*), SD3 [14] (checkpoint: *stabilityai/stable-diffusion-3-medium-diffusers*), SD3.5 [14] (checkpoint: *stabilityai/stable-diffusion-3.5-large*), SDXL [48] (checkpoint: *stabilityai/stable-diffusion-xl-base-1.0*), and LLM-based methods such as RPG [67]. We use *diffusers* [60] or official code to benchmark these models.

**Datasets.** We benchmark models on the widely used Visual Genome (VG) and the proposed MegaSG dataset.

- VG consists of 108k images annotated by human. Following SG2Im [27], it has been split into training set (62,565), validation set (5,506), and test set (5,088<sup>2</sup>) images for scene graph-based image generation.
- MegaSG comprises 1 million images annotated using Gemini 1.5 Flash. Relationships with a frequency below

<sup>2</sup>we use official code to obtain 5,096 images for test.

100 are filtered out, and synonyms are merged by a large language model (LLM).

**Metrics.** We employ common metrics and the proposed SGScore.

- Inception Score (IS) [53]: Measures the realism of generated images using a pre-trained Inception-V3 [57] network.
- Fréchet Inception Distance (FID) [22]: Assesses the similarity between generated and real images by measuring the distance between the distributions of their feature representations.
- CLIPScore [21]: Evaluates the semantic alignment between generated images and corresponding text using the CLIP model [49].
- SGScore measure the factual consistency in terms of object recall and relation recall. We use  $\alpha = 0.5$  in Eq. (4) of Section 3.2 to give a balanced measurement.

**Scene Graph Representation.** For text-to-image (T2I) models that condition on a sentence, we encode scene graphs in the format {subject} {predicate} {object} (e.g., cat sitting on desk, dog near chair). The prompt used to convert a scene graph into a consistent description (*i.e.*, the scene composition described in Section 4) is provided in Table 6.

**Scene Complexity.** We define the scene complexity of a scene graph  $G = (V, E)$  as:

$$C(G) = \gamma \cdot |V| + (1 - \gamma) \cdot |E|, \quad (6)$$

where  $\gamma$  is a weighting factor. The three levels of complexity are defined as follows:

- **Simple:**  $1 \leq C(G) \leq 3$ , typically involving 2–3 objects and no more than 3 relationships in the scene.
- **Medium:**  $4 \leq C(G) \leq 7$ , characterized by a denser arrangement of objects and relationships.
- **Hard:**  $C(G) \geq 8$ , representing the most challenging

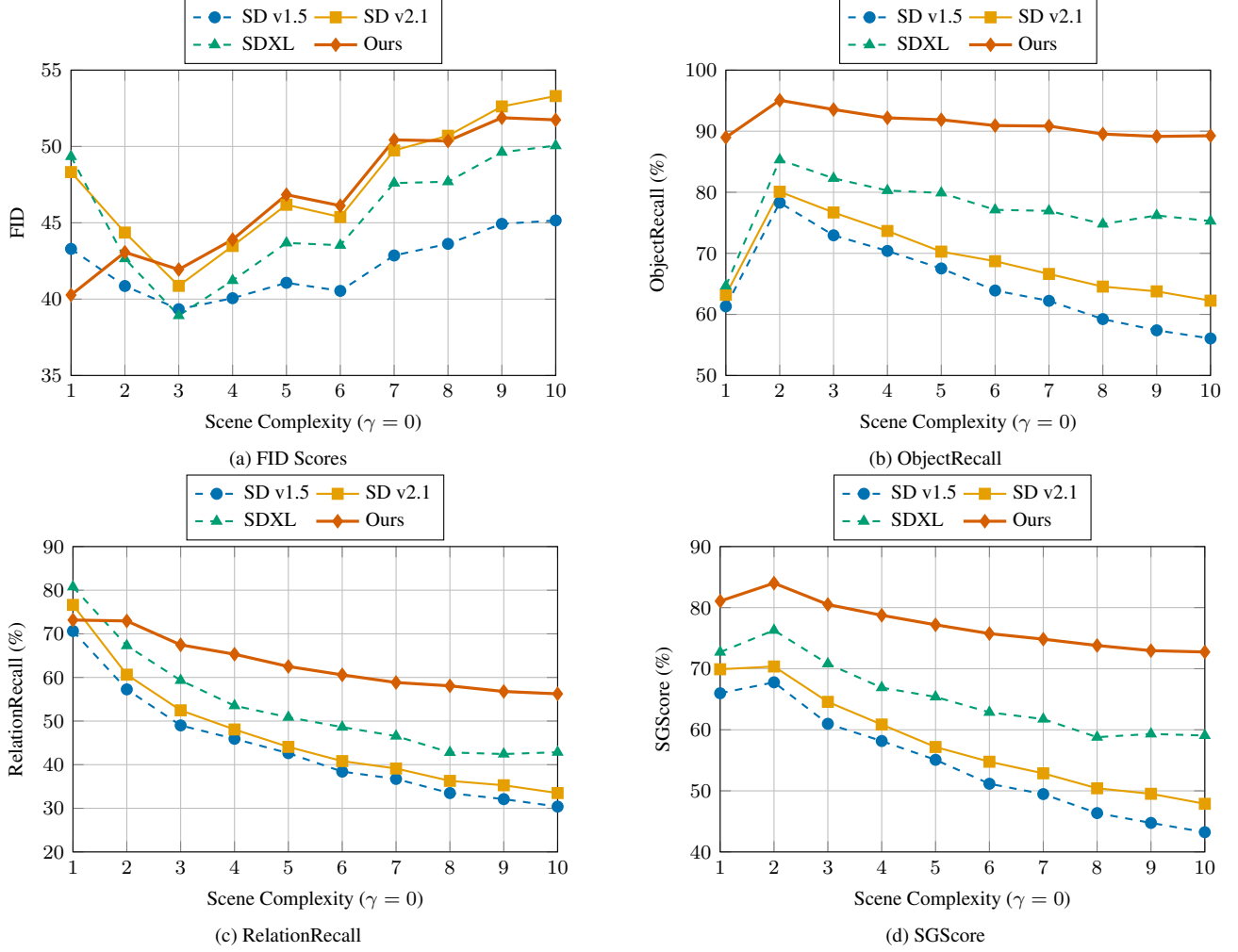


Figure 7. Comparison of FID, ObjectRecall, RelationRecall, and SGScore for models SD v1.5, SD v2.1, SDXL, and Ours across different scene complexity levels. (a) FID scores show relatively stable image quality, while (b) ObjectRecall and (c) RelationRecall indicate a consistent decline in factual consistency with increasing scene complexity. (d) SGScore demonstrates the overall advantage of our approach in maintaining higher factual consistency, particularly in complex scenes.

cases with highly dense objects and intricate relationships.

**LLM.** In addition to utilizing Gemini 1.5 Flash, we also present results using GPT-4o [1], Qwen-VL-Max [61], and LLaVA 1.5 [38] to evaluate the robustness of the proposed *SGScore*.

**IP-Adapter.** We use the official implementation in *diffusers* [60], with  $\lambda_0$  and  $\lambda_1$  (in Eq. (5) of Sec. 4) empirically set to 0.5.

## B.2. Evaluation of Scene-Bench

**Impact of Scene Complexity.** To examine how scene complexity affects model performance, we analyzed FID and SGScore for SD v1.5, SD v2.1, SDXL, and our model across various complexity levels (see Fig. 7).

As scene complexity increases (*i.e.*, with more objects and relationships), we observe a consistent decline in SGScore across all models. This suggests that, with greater complexity, the models struggle to accurately represent the expected scene graphs. The decreasing SGScore highlights the challenge of maintaining factual consistency in complex scenes. However, our model demonstrates a notable improvement over the other models by consistently achieving a higher SGScore across all complexity levels, particularly through maintaining stable and high object recall. This suggests that our model is more effective at preserving factual consistency even in complex scenes.

Interestingly, FID scores remain stable across complexity levels, indicating that image quality does not degrade significantly with complexity. This stability implies that

Select the candidate image that best matches the original image based on object alignment and relationships

Original Image



Candidates

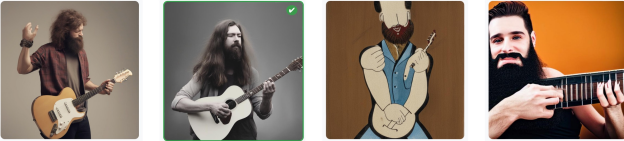


Select the candidate image that best matches the original image based on object alignment and relationships

Original Image



Candidates

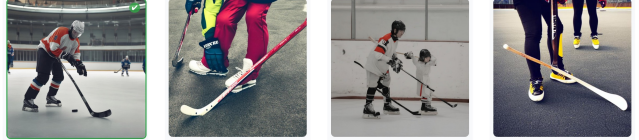


Select the candidate image that best matches the original image based on object alignment and relationships

Original Image



Candidates



Select the candidate image that best matches the original image based on object alignment and relationships

Original Image



Candidates



Figure 8. Example questions presented to human annotators.

while models retain visual fidelity, they encounter difficulties modeling intricate object relationships and interactions in complex scenes. Therefore, even as images appear visually coherent, the factual accuracy, as measured by SGScore, declines with increased scene complexity.

### B.3. Evaluation of Scene Graph Feedback

**Additional Ablation Study.** To evaluate the effectiveness of the scene graph feedback, particularly considering the additional parameters introduced by the IP-Adapter, we conducted another ablation study. In this experiment, we set  $\lambda_1 = 0$  in Eq. (5) of Sec. 4, meaning the IP-Adapter processes only the initial generated image, without incorporating the reference image derived from the missing graph.

As shown in Tab. 7, introducing the IP-Adapter alone (row 2 vs. row 1) does not improve the factual consistency of generated images. However, incorporating the reference image (row 3) significantly enhances ObjectRecall, RelationRecall, and SGScore, demonstrating the importance of scene graph feedback.

### B.4. Human Evaluation

We conducted a human evaluation to assess the effectiveness of SGScore in verifying factual consistency. Specifically, three human annotators were instructed to select the candidate image that best aligns with the original image regarding object presence and relationship accuracy. We randomly sampled 1,000 images and selected corresponding generated images from four models: SD v1.5, SD v2.1, SDXL, and Ours (SDXL). Model identities were hidden from the annotators to avoid bias. Fig. 8 illustrates the annotation interface.

## C. Additional Results

### C.1. Multimodal LLMs for SGScore

We evaluate the performance of different multimodal LLMs on SGScore, including Gemini 1.5 Flash [51], GPT-4o [1], Qwen-VL-Max [61], and LLaVA 1.5 [38], as shown in Fig. 11. The results show minimal discrepancies across



`messages = [ { "role": "user", "content": "You are an AI assistant tasked with converting scene graphs into descriptive text prompts for image generation using diffusion models. Given the input scene graph, generate a detailed text description adhering to the following instructions:`

`**Instructions:**`

1. **\*\*Scene Setup:\*\*** Begin by describing the overall setting or background of the scene. If no explicit background object exists, infer a suitable one from the present objects and relationships.
2. **\*\*Object Placement:\*\*** Introduce each object from the ‘objects’ list. When describing their placement, utilize the ‘relationships’ to accurately depict their positions relative to each other and the scene.
3. **\*\*Relationship Emphasis:\*\*** Vividly express the relationships between objects using descriptive language. Avoid simply stating the relationship; instead, showcase it through the objects’ placement, appearance, or actions.
4. **\*\*Image-ability:\*\*** Craft the description to be easily translatable into a visual representation. Use evocative language that captures the essence of the scene and guides the diffusion model.
5. **\*\*Conciseness and Clarity:\*\*** Be concise and avoid unnecessary details. Ensure the language is unambiguous and accurately reflects the scene graph information.

`**Output Format:**` Provide the output as a JSON object with a single key "description" and the value being the generated text description.

`**Input Scene Graph (JSON format):**`

````json {scene_graph} ````

`**Output:**` ` } ];`

`example_input = [ 'objects': ['cymbal.1', 'cymbal.2', 'drum.3', 'guitar.4', 'microphone.5', 'person.6'], 'relationships': [{ 'source': 'person.6', 'target': 'guitar.4', 'relation': 'playing' }, { 'source': 'person.6', 'target': 'microphone.5', 'relation': 'using' }, { 'source': 'guitar.4', 'target': 'cymbal.1', 'relation': 'near' }, { 'source': 'guitar.4', 'target': 'cymbal.2', 'relation': 'near' }, { 'source': 'guitar.4', 'target': 'drum.3', 'relation': 'near' } ]];`

`example_output= "A musician stands on a stage, the bright lights reflecting off their instruments. They are playing a guitar, their fingers dancing across the strings. A microphone is positioned in front of them, capturing their performance. The guitar rests near a pair of cymbals, and a drum sits nearby, adding to the musical ensemble."`

Table 6. Prompt for scene composition: translating a concise scene graph into a coherent and descriptive text.

IP-Adapter	Ref. Img.	ObjectRecall	RelationRecall	SGScore
✗	✗	75.45	48.84	62.14
✓	✗	70.91	49.83	60.37
✓	✓	<b>79.93</b>	<b>53.97</b>	<b>66.95</b>

Table 7. Comparison of ObjectRecall, RelationRecall, and SGScore with and without the reference image in the IP-Adapter setup. ‘Ref. Img.’ denotes the reference image.

models, indicating that SGScore is insensitive to the specific choice of state-of-the-art multimodal LLMs for the same evaluation. However, the visual reasoning capability of these models remains important. Considering cost-effectiveness, we recommend Gemini 1.5 Flash, which offers excellent multimodal reasoning performance at a significantly lower price [2], as indicated in Appendix D.4.

## C.2. More Qualitative Results

We present additional qualitative examples in Fig. 10, highlighting our model’s ability to handle complex scenes with multiple instances of the same object or relationship categories (1st row) as well as intricate indoor or outdoor scenes

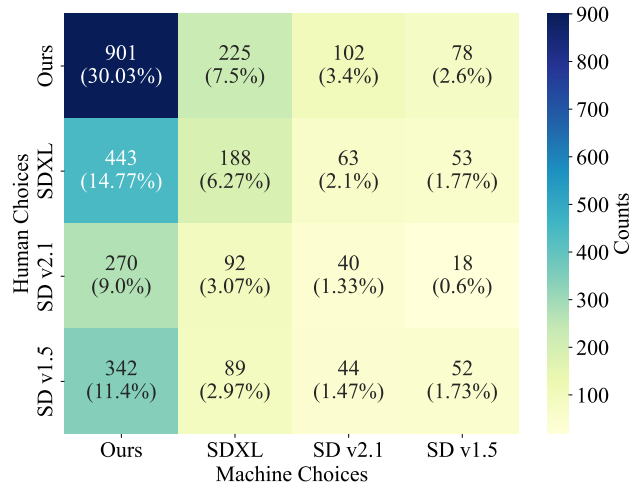


Figure 9. Confusion matrix showing the comparison of human choices against machine choices based on SGScore.

(2nd and 3rd rows). These results demonstrate our framework’s effectiveness in generating scene graph-guided images with high semantic fidelity.

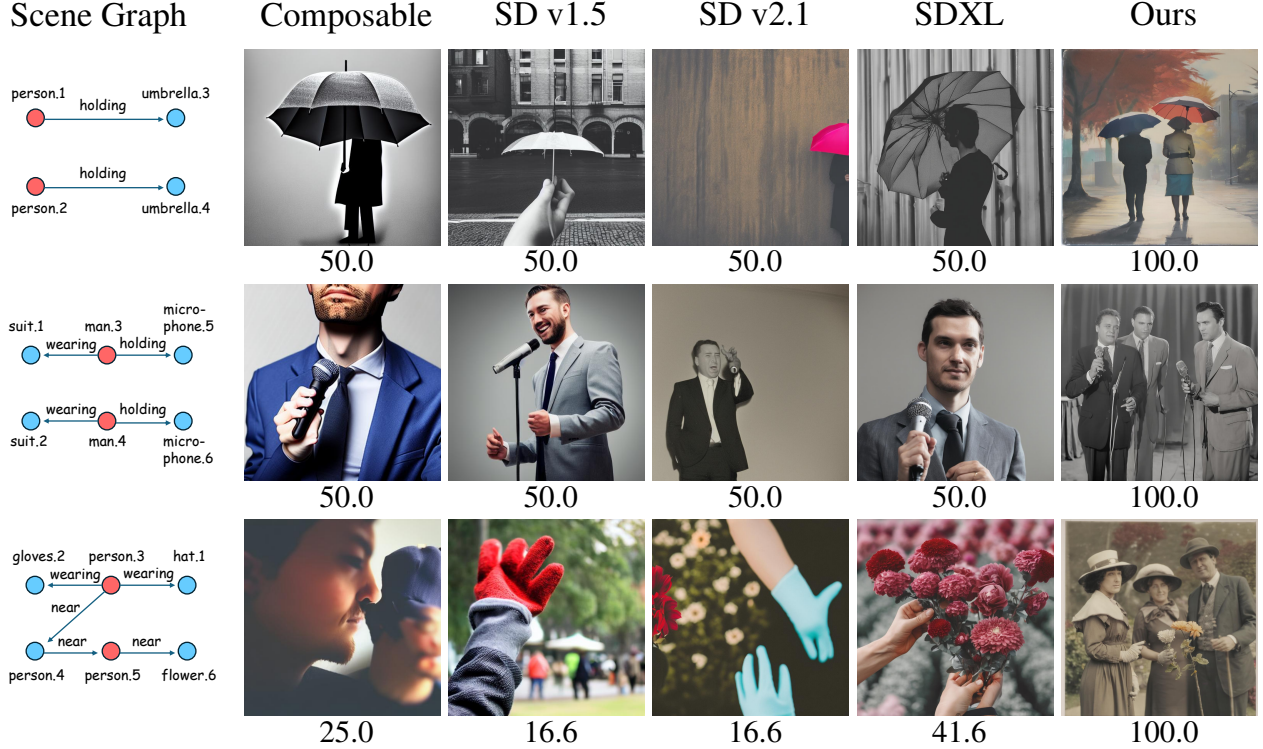


Figure 10. Comparison of Scene Graph-based Image Generation across Different Models. Each row displays a unique scene graph used as input for image generation. We present the **SGScore** below each generated image to quantify the consistency between the scene graph and the generated output.

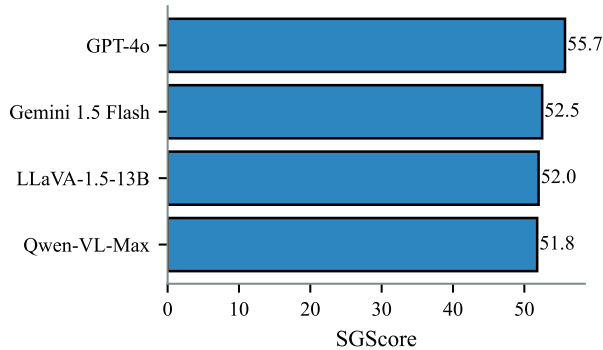


Figure 11. Performance comparison of M-LLMs on VG test set (images are generated by SD v1.5).

## D. Discussion

### D.1. Sensitivity Analysis of SGScore

To test the scalability and sensitivity of SGScore, we randomly sample subsets (e.g., with size 500, 1k, 2k, 4k, ..., 32k, etc.) from the MegaSG to compute the SGScore on images generated by SD v1.5. As shown in Fig. 12, the mean SGScore remains relatively stable across sample sizes, with

only slight variations observed. Additionally, the standard deviation decreases as the sample size increases, demonstrating that the metric becomes more reliable and less sensitive to random fluctuations with larger subsets. This indicates that SGScore is both scalable and robust, providing consistent evaluations of factual consistency regardless of the dataset size.

### D.2. Do We Really Need Attributes for SG2IM?

One potential concern for *MegaSG* is its lack of attribute annotations, as users might expect attributes to play a role in scene generation—for example, distinguishing between a red apple is above the black car and a black apple is above the red car. Does omitting attributes in *MegaSG* adversely affect the modeling of such distinctions?

Recent work [13] demonstrates that diffusion models can effectively bind attributes (e.g., color, texture, shape) under certain conditions. However, most existing SG2IM approaches [16, 27, 40, 56, 66] do not explicitly model attributes, despite their availability in the Visual Genome dataset. To evaluate the impact of attribute modeling, we augment 775 object categories in *MegaSG* with attribute labels (e.g., {apple → red apple, green apple, ripe apple},

```

messages = [{ "role": "user", "content": "Given a file listing object categories, generate 3 realistic instances
for each category by adding common-sense visual attributes such as color, size, material, or texture. Ensure that the at-
tributes are contextually appropriate. For example, transform 'apple' into 'red apple', 'green apple', and 'ripe apple'; or
'car' into 'white car', 'small car', and 'luxury car'. The generated instances should be diverse and plausible. formulate
the output as a dict in JSON like {"apple": ["red apple", "green apple", "ripe apple"], "car": ["white car", "black car",
"luxury car"]} } ];

```

Table 8. Prompt for refining object categories with attributes. The LLM receives a list of object categories as input and outputs corresponding fine-grained object descriptions.

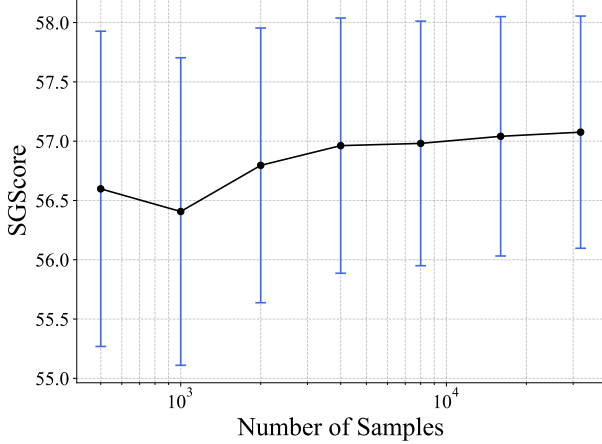


Figure 12. Mean and standard deviation (std.) of SGScore across varying numbers of samples. For each sample size, the image generation process is repeated with different random seeds using SD v1.5 to compute the mean and std. of SGScore.

{*door* → *wooden door*, *red door*, *glass door*}, etc.). Each object category is augmented three times by a multimodal LLM (the prompt can be found in Tab. 8), yielding a total of 2,325 text prompts for diffusion models. As shown in Table 9, diffusion models consistently handle both single-object and attribute-bound object generation with minimal performance differences, suggesting that explicit attribute modeling offers only marginal benefits in this setting.

More importantly, our experiments (e.g., Tab. 4 and Fig. 7) reveal that current diffusion models struggle to capture spatial and interactive relationships, rather than merely modeling individual objects. This shortcoming can be attributed to two factors. First, T2I models typically employ a CLIP text encoder to process the textual input; however, due to dataset biases (e.g., LAION 5b [54]) during training, the encoder learns a visual-text alignment that favors object presence over the relationships between objects. Similarly, the training data for Stable Diffusion models predominantly consists of single-object images, providing limited exposure to the alignment of multiple objects and their interactions.

Considering the trade-off between annotation cost and the minimal gains from introducing attributes, we opted to

	SD v1.5	SDXL
w.o. attributes	93.90 ± 0.29	92.40 ± 0.36
w. attributes	90.12 ± 0.26	93.34 ± 0.15

Table 9. Recall comparison of single-object vs. attribute-bound generation on 775 object categories. The recall evaluation is performed by Gemini 1.5 Flash.

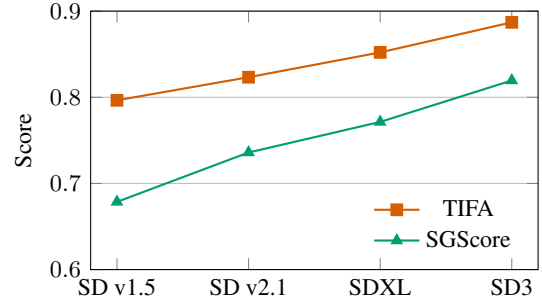


Figure 13. Comparison of TIFA and SGScore across different Stable Diffusion models on TIFA v1.0 benchmark.

omit attributes in the construction of *MegaSG*. Our focus is on effectively evaluating scene graph-to-image generation (SG2IM), thus providing a promising direction for optimizing diffusion models.

### D.3. Compared to Existing Benchmarks

Although our work focuses on Scene Graph-to-Image (SG2IM) generation, textual inputs can be directly parsed into structured scene graphs. To validate the effectiveness of our proposed *SGScore* in enhancing factual consistency, we compare *SGScore* with two text-to-image (T2I) benchmarks, namely TIFA [24] and DSG [12].

TIFA [24] examines faithfulness in Visual Question Answering (VQA) by leveraging GPT-3 [5] for question generation and using question answering modules such as mPLUG [34] and BLIP-2 [36]. It also introduces the TIFA v1.0 benchmark, which comprises 4,081 text prompts. With these text prompts, we synthesize images using different diffusion models to compare *SGScore* with the TIFA score, evaluated using the mPLUG-large model. To com-

```

messages = [{ "role": "user", "content": "Extract a structured scene graph from the following sentence. In
this scene graph, include all physical objects even if they do not participate in any relationships (i.e., allow orphan
nodes). The output should be a dictionary with two keys: - "objects": a list of all physical objects mentioned in the
sentence. - "relationships": a list of dictionaries, each containing: - "source": the subject (a physical object) of the
relationship. - "target": the object (a physical object) of the relationship. - "relation": the predicate describing the
relationship between the source and target. Ensure that both "source" and "target" are physical objects (not abstract
concepts).
Sentence: "{input_sentence}"
Output format: { "objects": [ ... ], "relationships": [ "source": "...", "target": "...", "relation": "...", ... ] }
];

```

Table 10. Prompt for extracting a textual scene graph from a caption.

pute *SGScore*, we utilize an LLM (e.g., Gemini 1.5 Flash) with the prompt detailed in Tab. 10 to extract a textual scene graph from a caption. From Fig. 13, we observe a consistent trend between the TIFA score and *SGScore* across different diffusion models on the TIFA v1.0 benchmark, indicating that both metrics reliably reflect factual consistency. However, while TIFA is designed for text-to-image (T2I) generation, our *SGScore* focuses on scene graph-to-image (SG2IM) generation.

Similarly, DSG [12] decomposes the text prompt into a series of tuples (e.g., entities, attributes, relations) and generate corresponding questions for verifying the faithfulness of text-to-image generation. However, due to the high computational cost (see Appendix D.4), we opted not to report DSG scores against TIFA and *SGScore*.

#### D.4. Computation Cost

**Computation cost for evaluation pipeline.** We benchmark 5,000 samples using Gemini 1.5 Flash to assess computation cost. On average, input and output token consumption are  $\sim 4.7\text{M}$  and  $\sim 3.9\text{M}$ , respectively, with a cost of  $\sim 1.5$  USD for 5k samples (as of March 2025)<sup>3</sup>. In contrast, DSG [12] requires  $\sim 45\text{M}$  input tokens and  $\sim 0.7\text{M}$  output tokens, resulting in a cost of  $\sim 7$  USD for benchmarking 5k samples—even when using the considerably cheaper and more powerful LLM model GPT-4o mini [46] compared to the originally employed `gpt-3.5-turbo-16k-0613` in the paper.

**Computation cost for scene graph feedback.** While scene graph feedback can be iteratively applied to refine generated results, we perform a single refinement step once discrepancies are detected by our evaluation pipeline. As shown in Tab. 3 and Tab. 2, this approach yields a significant performance gain despite the additional computational overhead. A related work in T2I generation [63] also employs an iterative correction pipeline, integrating an object detector with an LLM, which requires extra computational cost.

<sup>3</sup>Gemini API pricing [2]